JCI The Journal of Clinical Investigation

RASAL2 activates RAC1 to promote triple-negative breast cancer progression

Min Feng, … , Dave S.B. Hoon, Qiang Yu

J Clin Invest. 2014;124(12):5291-5304. https://doi.org/10.1172/JCI76711.

Research Article **Oncology**

Patients with triple-negative breast cancer (TNBC) have a high incidence of early relapse and metastasis; however, the molecular basis for recurrence in these individuals remains poorly understood. Here, we demonstrate that *RASAL2*, which encodes a RAS-GTPase–activating protein (RAS-GAP), is a functional target of anti-invasive microRNA-203 and is overexpressed in a subset of triple-negative or estrogen receptor–negative (ER-negative) breast tumors. As opposed to luminal B ER-positive breast cancers, in which RASAL2 has been shown to act as a RAS-GAP tumor suppressor, we found that RASAL2 is oncogenic in TNBC and drives mesenchymal invasion and metastasis. Moreover, high RASAL2 expression was predictive of poor disease outcomes in patients with TNBC. RASAL2 acted independently of its RAS-GAP catalytic activity in TNBC; however, RASAL2 promoted small GTPase RAC1 signaling, which promotes mesenchymal invasion, through binding and antagonizing the RAC1-GAP protein ARHGAP24. Together, these results indicate that activation of a RASAL2/ARHGAP24/RAC1 module contributes to TNBC tumorigenesis and identify a context-dependent role of *RASAL2* in breast cancer.

Find the latest version:

https://jci.me/76711/pdf

RASAL2 activates RAC1 to promote triple-negative breast cancer progression

Min Feng,[1] Yi Bao,[1] Zhimei Li,[1] Juntao Li,[2] Min Gong,[1] Stella Lam,[3] Jinhua Wang,[3] Diego M. Marzese,[3] Nicholas Donovan,[3] Ern Yu Tan,[4] Dave S.B. Hoon,[3] and Qiang Yu[1,5,6]

[1]Cancer Therapeutics and Stratified Oncology and [2]Computational Biology, Genome Institute of Singapore, Agency for Science, Technology, and Research (A*STAR), Biopolis, Singapore. [3]Department of Molecular Oncology, John Wayne Cancer Institute, Santa Monica, California, USA. [4]Department of General Surgery, Tan Tock Seng Hospital, Singapore. [5]Department of Physiology, Yong Loo Lin School of Medicine, National University of Singapore, Singapore. [6]Cancer and Stem Cell Biology, DUKE-NUS Graduate Medical School of Singapore, Singapore.

Patients with triple-negative breast cancer (TNBC) have a high incidence of early relapse and metastasis; however, the molecular basis for recurrence in these individuals remains poorly understood. Here, we demonstrate that *RASAL2*, which encodes a RAS-GTPase–activating protein (RAS-GAP), is a functional target of anti-invasive microRNA-203 and is overexpressed in a subset of triple-negative or estrogen receptor–negative (ER-negative) breast tumors. As opposed to luminal B ER-positive breast cancers, in which RASAL2 has been shown to act as a RAS-GAP tumor suppressor, we found that RASAL2 is oncogenic in TNBC and drives mesenchymal invasion and metastasis. Moreover, high RASAL2 expression was predictive of poor disease outcomes in patients with TNBC. RASAL2 acted independently of its RAS-GAP catalytic activity in TNBC; however, RASAL2 promoted small GTPase RAC1 signaling, which promotes mesenchymal invasion, through binding and antagonizing the RAC1-GAP protein ARHGAP24. Together, these results indicate that activation of a RASAL2/ARHGAP24/RAC1 module contributes to TNBC tumorigenesis and identify a context-dependent role of *RASAL2* in breast cancer.

Introduction

Triple-negative breast cancer (TNBC), characterized by tumors that do not express estrogen receptor (ER), progesterone receptor (PR), or human epidermal growth factor receptor 2 (HER2), represents the most aggressive subtype of breast cancer, with a high rate of relapse and no available therapeutic targets (1, 2). Currently, chemotherapy is the main treatment modality for TNBC, but one-third of patients develop recurrence within 3 years of adjuvant therapy (3). One important goal of research is to identify novel prognostic biomarkers that can reliably stratify patients with TNBC according to clinical outcomes. This, however, has been hampered by a lack of understanding of the mechanisms underlying distant metastasis and early relapse in TNBC.

Among the many proposed mechanisms underlying metastasis (4, 5), microRNA-regulated (miRNA-regulated) transcriptional dynamics has emerged as a critical step (6). In human cancers, many miRNAs act as potential tumor suppressors and their downregulation leads to overexpression of cancer-promoting genes (7–9). Several miRNAs known to target and suppress invasion and metastasis are often found to be downregulated in breast cancers, consistent with a role in breast cancer progression (8, 10–14). These anti-invasive miRNAs suppress breast cancer cell invasiveness through various mechanisms. For example, members of the miR-200 family seem to inhibit the expression of genes associated with epithelial-to-mesenchymal transition (EMT) (15–17), a step considered critical for metastatic dissemination (18), while miR-126 and miR-126* modulate the tumor stromal microenvironment to inhibit cellular invasion (14, 19). Other miRNAs like miR-708 can attenuate metastasis by targeting the endoplasmatic reticulum and intracellular calcium levels (20). Here, we describe miRNA-203 as a key anti-invasive miRNA downregulated in TNBC and identify *RASAL2* as a clinically relevant downstream target, with a critical role in promoting invasion and metastasis in TNBC.

Results

RASAL2 is a target of anti-invasive miR-203 and is overexpressed in TNBC or ER-negative tumors. As it has been found that anti-invasive miRNAs are often downregulated in TNBC, we therefore profiled the global miRNA expression in 2 highly invasive TNBC cell lines (MDA-MB-231 and BT-549) in comparison with that in 2 noninvasive luminal-type breast cancer cell lines (MCF-7 and BT474). Fifty-four miRNAs were found to be significantly downregulated in both TNBC cell lines as compared with the 2 luminal lines (using 3-fold cutoff, $P < 0.01$; Supplemental Table 1; supplemental material available online with this article; doi:10.1172/JCI76711DS1). The top 10 miRNAs are shown in the expression heat map shown in Figure 1A. Among them are the 5 members of miR-200 family (miR-200a/b/c, miR-141, and miR-429), which is known to be anti-invasive by targeting and inhibiting EMT-promoting transcription factors such as ZEB1/2 (16, 17). We also found that miR-203 was among the most downregulated in TNBC cells. Although recent studies have indicated a tumor-suppressive role for miR-203 in several cancers types, including breast cancer (21–23), its functional targets in regulating breast cancer invasion have yet to be identified. In this study, we have chosen to focus on miR-203, with the objective to elucidate its targets that may have functions in TNBC tumorigenesis.

Conflict of interest: The authors have declared that no conflict of interest exists.
Submitted: April 21, 2014; **Accepted:** October 14, 2014.
Reference information: *J Clin Invest*. 2014;124(12):5291–5304. doi:10.1172/JCI76711.

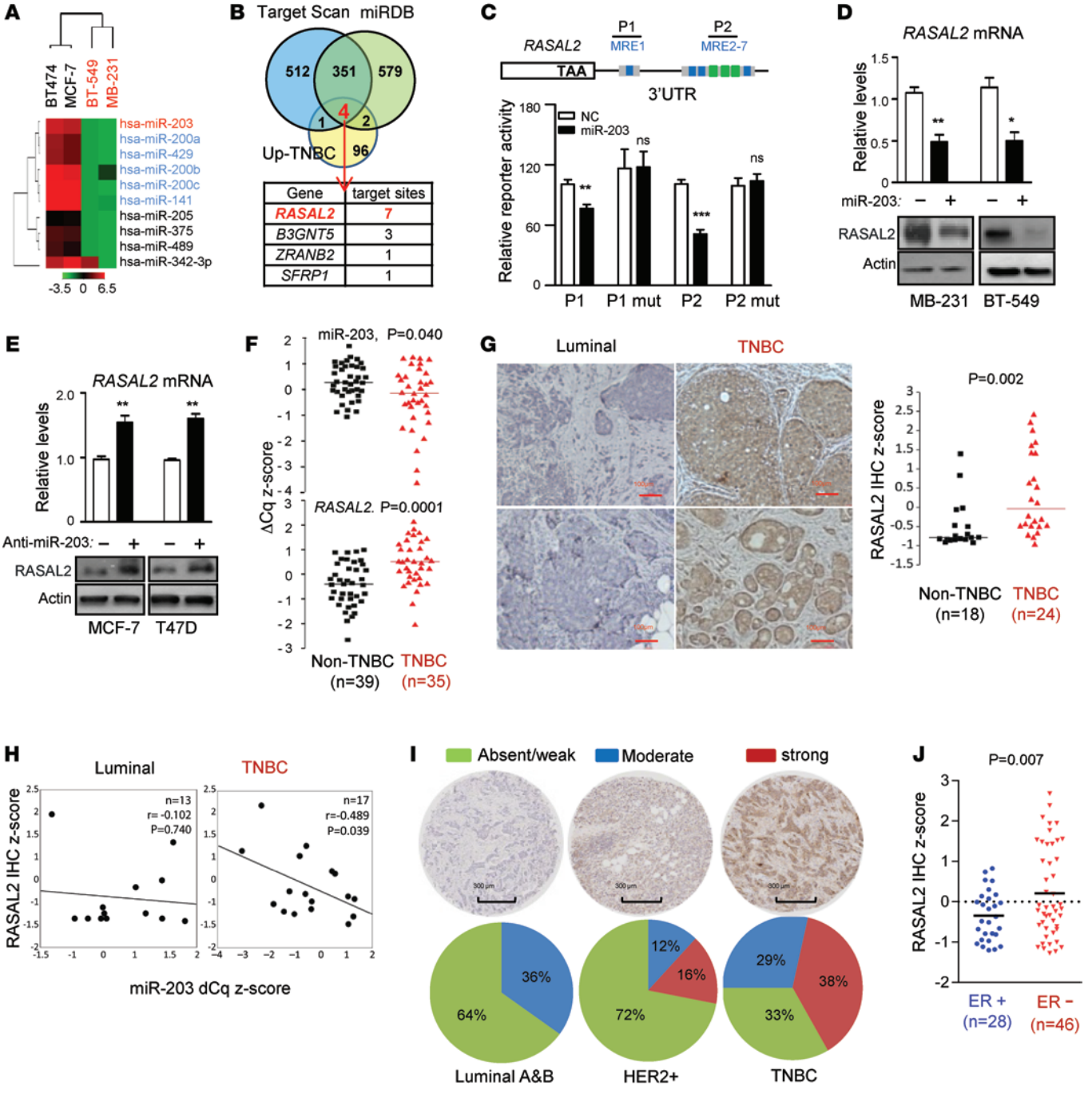

Figure 1. miRNA and mRNA profiling identifies concurrent deregulations of miR-203 and *RASAL2* in TNBC. (**A**) Heat map of miRNA profiling showing the 10 top-ranked downregulated miRNAs in indicated cell lines. (**B**) Venn diagram of putative miR-203 target genes predicted by TargetScan and miRDB algorithms and the 103 TNBC upregulated genes identified previously (24) in addition to the 4 genes that overlap, with number of putative miR-203 target sites. (**C**) The diagram shows the 2 regions containing miR-203–binding sites (a single miRNA recognition element [MRE] in P1 and 6 MREs [MRE2–MRE7] in P2) of the luciferase reporter construct of the 3′ UTR of *RASAL2*. Reporter activity was normalized to wild-type reporter activity in cells expressing a nontargeting control (NC) microRNA. (**D**) qPCR and Western blot analysis of *RASAL2* levels in MDA-MB-231 and BT-549 cells treated with miR-203 mimics. (**E**) qPCR and Western blot analysis of *RASAL2* levels in MCF-7 and T47D cells treated with miR-203 antagomir inhibitor. (**F**) qPCR analysis of miR-203 and *RASAL2* in breast tumor specimens. ΔCq, quantification cycle. (**G**) Representative images and quantification of IHC staining for RASAL2 in luminal or TNBC tumors. (**H**) Correlation analysis of RASAL2 and miR-203 in luminal and TNBC tumors expressing high (upper quartile) and low (lower quartile) levels of miR-203. (**I**) IHC analysis of the TMA cohort, showing the percentages of staining of different tumor subtypes (strong [67%–100%], moderate [34%–66%], or absent/weak [0%–33%]) for RASAL2 protein. (**J**) Scatter plot showing RASAL2 protein expression in indicated breast tumors. The data shown represent mean ± SEM of 3 independent experiments. Scale bar: 100 μm (**G**); 300 μm (**I**). $^{*}P \le 0.05$, $^{**}P \le 0.01$, $^{***}P \le 0.001$.

To search for putative targets of miR-203, we used TargetScan (http://www.targetscan.org) and miRDB (http://mirdb.org) computational tools and identified a common set of 355 candidate genes whose 3′ untranslated regions (3′ UTRs) contain at least one putative miR-203–binding sequence (Figure 1B). A comparison of these candidate genes with a list of 103 genes that were previously identified as being overexpressed in both TNBC cell lines and clinical samples (24) revealed 4 putative miR-203 targets that are upregulated in TNBC (Figure 1B). Of these, *RASAL2*, which encodes the RAS protein activator like 2, a putative RAS-GTPase–activating protein (RAS-GAP), emerged as a top candidate whose 3′ UTR contains 7 putative miR-203–binding sites (Figure 1B), including 3 that are highly conserved (Supplemental Figure 1A).

To validate *RASAL2* as a direct target of miR-203, we performed the 3′ UTR luciferase reporter assay using 2 pMIR-REPORT constructs: one containing the first miR-203–binding site (P1) and the other containing the remaining 6 sites that are closely clustered together in an 1,173-bp region (P2) (Figure 1C). The results showed that the ectopic miR-203 was able to repress the luciferase activity of both P1 and P2 constructs but not that of the constructs in which the respective miR-203–binding sites were mutated, supporting a direct interaction of miR-203 with *RASAL2* 3′ UTR (Figure 1C). Furthermore, ectopic expression of miR-203 in the TNBC MDA-MB-231 and BT-549 cells markedly reduced *RASAL2* expression at both mRNA and protein levels (Figure 1D). Conversely, a synthetic antagomir inhibitor of miR-203 increased *RASAL2* expression in luminal MCF-7 and T47D cells but not TNBC MDA-MB231 and BT-549 cells (Figure 1E and Supplemental Figure 1B). Together, these results support *RASAL2* as a direct target of miR-203.

Using quantitative PCR (qPCR) and Western blotting in a panel of breast cancer cell lines, we confirmed the downregulation of miR-203 and the upregulation of *RASAL2* in TNBC lines as compared with that in non-TNBC lines (Supplemental Figure 1C). Importantly, in clinical tissue specimens we confirmed the significant downregulation of miR-203 and upregulation of *RASAL2* in TNBC tumors compared with that in non-TNBC tumors (Figure 1F).

Expanded analyses using public databases, including GOBO (25), Oncomine (26), and The Cancer Genome Atlas (TCGA), have further confirmed *RASAL2* upregulation in basal or TNBC cell lines and clinical samples, both in a panel of 55 breast cancer lines (Supplemental Figure 2, A and B) and in multiple clinical data sets (Supplemental Figure 2C). Of significant note, the TCGA analysis revealed a step-wise upregulation of *RASAL2* toward aggressiveness, showing the highest expression in basal tumors, followed by HER2$^+$ tumors and luminal tumors (Supplemental Figure 2D), in which *RASAL2* was found to be strongly upregulated in approximately 31% of basal tumors (which often overlapped with TNBC tumors) compared with <6% in luminal tumors (Supplemental Figure 2E). TCGA analysis also revealed a potential *RASAL2* gene amplification in a small set of basal tumors (4.9%) (Supplemental Figure 2E, top), indicating a possible alternative mechanism for *RASAL2* upregulation.

Finally, RASAL2 protein level expression in clinical tissue specimens was evaluated by immunohistochemistry (IHC) analysis with a RASAL2 antibody whose specificity has been experimentally validated (Supplemental Figure 3). Consistent with the mRNA analysis, RASAL2 protein was found to be expressed at significantly higher levels in TNBC tumors compared with that in non-TNBC tumors (Figure 1G). Moreover, in patient samples expressing high and low levels of miR-203 we identified a significant inverse correlation between miR-203 and RASAL2 in TNBC tumors but not luminal tumors (Figure 1H).

The IHC result was further validated and expanded using a breast tissue microarray (TMA) that contained 74 breast cancer specimens of different subtypes. By using a cutoff to score strong, moderate, or weak levels of staining, we showed that RASAL2 was expressed strongly in 38% of TNBC tumors and 16% of HER2$^+$ tumors but had little or no expression in luminal tumors (Figure 1I). Of note, the IHC staining was also able to show the striking difference in RASAL2 expression just based on the ER status (Figure 1J).

RASAL2 expression is positively associated with poor clinical outcomes, early metastasis, and disease recurrence in basal or ER-negative patients. To assess the clinical role of *RASAL2* deregulation in breast cancer, we performed Kaplan-Meier meta-analyses using the GOBO online database (http://co.bmc.lu.se/gobo/), which consists of 10 breast cancer cohorts and 1,789 patients. In both overall survival and early distant metastasis and relapse-free survival analysis (within 5 years), we found that *RASAL2* expression level was not prognostic in unselected patients (all patients), but an expression level in the top 30% was significantly associated with the poor outcomes in patients with basal tumors (which overlap largely with TNBC tumors though are not completely equivalent) and showed an opposite trend in patients with luminal tumors, as stratified based on the PAM50 gene signature (Figure 2, A and B, and ref. 27).

We next asked whether breast cancer stratification by just ER status is sufficient to demonstrate the prognostic value of *RASAL2*. The results showed that *RASAL2* high expression was consistently associated with poor overall or metastasis- and relapse-free survivals in ER-negative patients, while they again showed an opposite trend in patients with ER-positive tumors (Figure 2C). Moreover, in the multivariate analysis, *RASAL2* emerged as a stand-alone predictor of prognosis in ER-negative tumors (for tumors with low *RASAL2* expression, hazard ratio = 0.47; $P = 0.03$), independent of other clinical parameters (Figure 2D). Thus, the role of *RASAL2* in breast cancer seems to be context dependent: it is oncogenic in basal/TNBC or ER-negative tumors but can function as a tumor suppressor in luminal tumors. Indeed, the latter is consistent with a recent report showing a tumor-suppressive role of *RASAL2* in luminal B breast cancers (28).

To further assess the role of *RASAL2* in breast cancer metastasis progression, we analyzed RASAL2 expression using a breast cancer TMA containing tissue cores from 36 paired, localized primary tumors and matched lymph node metastasis specimens. IHC staining of ER expression in these tumor specimens showed 11 of 36 patients as ER positive and 25 of 36 as ER negative (using 5% ER positivity as a cutoff point). We found that 18 of 25 ER-negative tumors (72%) showed marked upregulation of RASAL2 in node metastasis compared with the primary tumors ($P < 0.001$), while the corresponding changes in ER-positive tumors seemed to be random and not significant ($P = 0.77$) (Figure 2E). This supports a role of RASAL2 in metastatic tumor progression in ER-negative tumors.

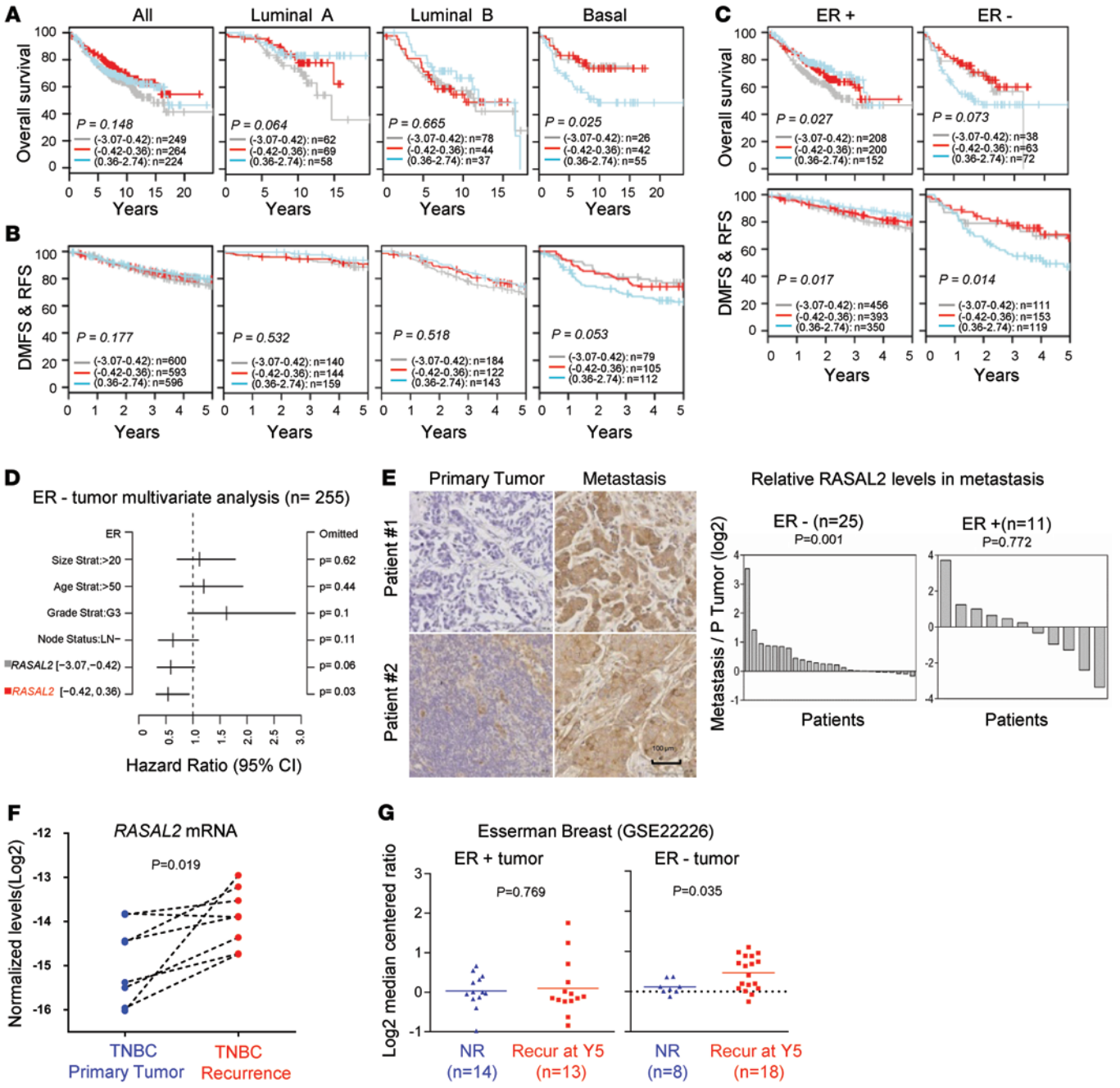

Figure 2. *RASAL2* overexpression is associated with poor disease outcome, metastasis, and tumor recurrence in TNBC or ER-negative tumors. (**A** and **B**) Kaplan-Meier analyses of overall survival and early distance metastasis combined with relapse-free survival (DMFS & RFS), respectively, using the GOBO database. Patients were stratified according PAM50 subtypes as indicated. (**C**) Similar analysis as in **A** and **B**, but patients were stratified according ER status as indicated. (**D**) Multivariate analysis of ER-negative tumors in the patients in **C**. (**E**) IHC staining of RASAL2 on primary tumors and matched node metastasis specimens from 2 representative patients as well as the relative RASAL2 expression in metastatic tumors relative to that in paired primary tumors in a TMA comprising 25 ER-negative and 11 ER-positive patients. ER positivity was determined by IHC using 5% ER-positive cells as a cutoff point. Data were analyzed using a paired 2-tailed t-test and are reported as mean ± SEM. Scale bar: 100 μm. (**F**) qPCR analysis of *RASAL2* mRNA expression levels in a group of paired primary and recurrent TNBC tumors (n = 8). Blue dots represent individual primary tumors, red dots represent recurrent tumors after surgery and chemotherapy, and dotted lines connect data from individual patients. (**G**) Stratified analysis of data from Esserman (ref. 29; GEO accession no. GSE22226), correlating *RASAL2* levels with 5-year (recur at 5Y) recurrence incidence in ER-positive or ER-negative groups of patients. NR, no recurrence.

We next analyzed a set of TNBC primary tumors and matched recurrent tumors following the chemotherapy. qPCR analysis showed higher levels of *RASAL2* expression in most of the recurrent tumors compared with that in the matched primary tumors (Figure 2F), revealing a role of *RASAL2* in TNBC tumor recurrence. Moreover, by analyzing the gene expression data associated with breast cancer chemoresistance and recurrence in the I-SPY 1 TRIAL (29), we observed that patients with

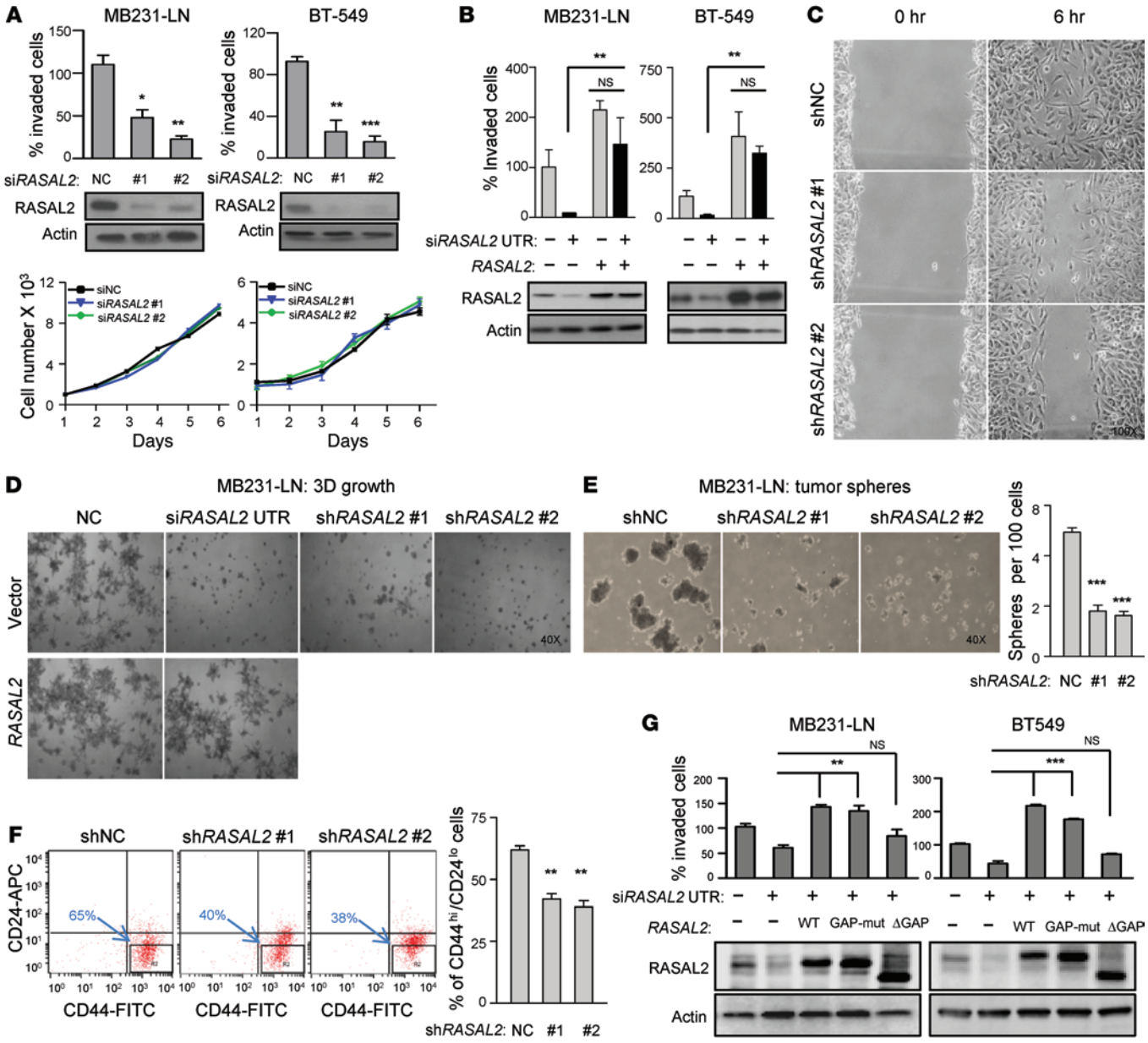

Figure 3. *RASAL2* knockdown inhibits TNBC invasion and aggressive growth. (**A**) Effects of 2 independent *RASAL2* siRNAs on cell invasion, RASAL2 protein expression levels, and monolayer cell proliferation. (**B**) Invasion assay and RASAL2 protein levels in cells expressing ectopic *RASAL2* treated with a siRNA targeting the 3′ UTR of *RASAL2*. (**C**) Wound healing assay of a confluent culture of indicated MB231-LN cells at hour 0 of wound scratching and 6 hours after scratching on collagen I–coated plates. (**D**) Representative images of cell growth in 3D Matrigel. MB231-LN cell lines were treated as indicated. (**E**) Representative images and quantification of the number of tumorspheres formed per 100 MB231-LN cells as indicated. (**F**) Representative images and quantification of $CD44^{hi}CD24^{lo}$ cells in MB231-LN cells treated as indicated. (**G**) Invasion assay and RASAL2 protein levels in cells expressing ectopic wild type, GAP activity–deficient mutant (GAP-mut), or GAP domain deletion mutant (ΔGAP) RASAL2 treated with a siRNA targeting the 3′ UTR of *RASAL2*. The data shown represent mean ± SEM of 3 independent or replicate experiments. Original magnification, ×100 (**C**); ×40 (**D** and **E**). $^*P < 0.05$, $^{**}P < 0.01$, $^{***}P < 0.001$.

recurrent tumors had higher levels of *RASAL2* in their primary tumors; importantly, this upregulation of *RASAL2* upon recurrence was only seen in ER-negative tumors ($P = 0.035$) and not in ER-positive tumors ($P = 0.77$) (Figure 2G). Collectively, these clinical data further support the oncogenic role of *RASAL2* in TNBC or ER-negative tumors.

It has been shown recently through large-scale genomic analysis that TNBC and high-grade serous ovarian cancers showed a remarkable similarity in the molecular portraits (30). We next asked whether *RASAL2* has a similar oncogenic role in high-grade ovarian cancer. Intriguingly, by Oncomine analysis, we found that *RASAL2* was markedly upregulated in high-grade serous ovarian cancer in both mRNA levels and gene copy numbers (Supplemental Figure 4, A and B). This was further confirmed by IHC analysis using a commercial ovarian cancer TMA (Supplemental Figure 4C). Moreover, *RASAL2* expression showed a progressive upregulation toward metastasis in Fédération Internationale de Gynécologie Obstétrique staging analysis of the Meyniel ovarian data set (Supplemental Figure 4D and

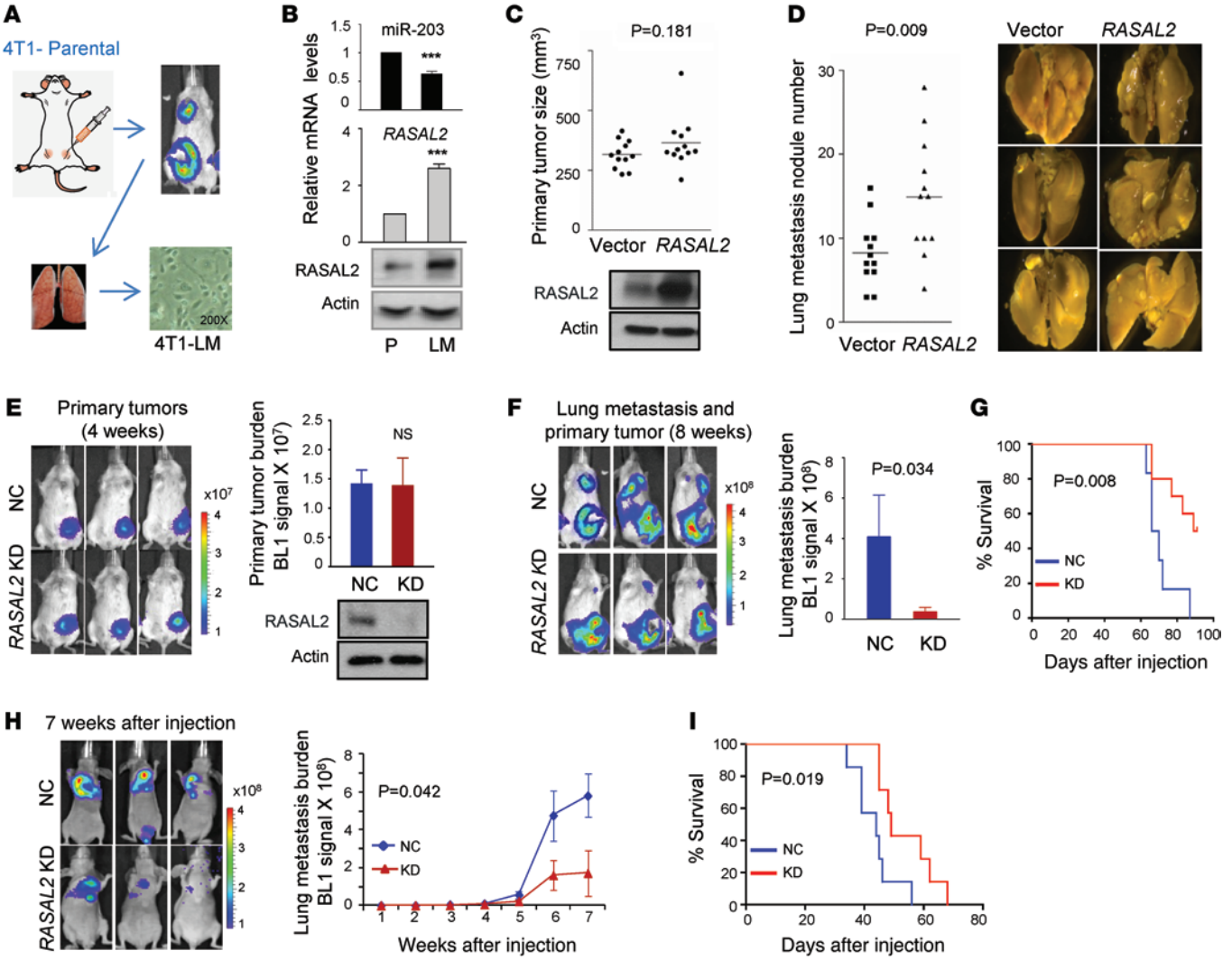

Figure 4. Role of *RASAL2* in TNBC metastasis in vivo. (**A**) Schematic of ex vivo analysis of parental 4T1 cells and a lung metastatic subline (4T1-LM). Original magnification, ×100. (**B**) qPCR analysis of miR-203, *RASAL2* mRNA, and protein levels of indicated cells. (**C**) Primary tumor size after orthotopic injection of mammary fat pads with 4T1 control cells (Vector) and 4T1 cells expressing ectopic RASAL2 as well as RASAL2 Western blot. (**D**) The number of lung metastasis nodules from spontaneous metastasis after orthotopic injection of 4T1 cells and an image of whole lung 4 weeks after injection. (**E**) Representative bioluminescence (BLI) images of female NOD/SCID mice showing the primary tumors at week 4 derived from orthotopic injection of MB231-LN control cells (NC) and *RASAL2* deleted cells by shRNA (KD) and quantification of the primary tumor (n = 16). (**F**) Representative bioluminescence images of female NOD/SCID mice showing both the primary tumors (hind leg) and metastasis (lung) derived from orthotopic injection of MB231-LN cells with control and *RASAL2* KD treatment at week 8. Quantification of the pulmonary metastases by bioluminescence measurement (n = 16). (**G**) Kaplan-Meier curves of mice from **E** and **F** (n = 16). Curves were compared using a log-rank (Mantel-Cox) test. P = 0.008. (**H**) Representative bioluminescence images of lung metastasis development in female NOD/SCID mice injected via lateral tail vein with control and *RASAL2* KD cells and quantification of pulmonary metastases by bioluminescence measurement (n = 16). (**I**) Kaplan-Meier curves of mice from **H** (n = 16). Curves were compared using a log-rank (Mantel-Cox) test. P = 0.019.

ref. 31). Finally, high *RASAL2* expression was consistently associated with poorer disease outcomes in multiple cohorts of ovarian cancer (Supplemental Figure 4E). These data support a role of *RASAL2* in high-grade serous ovarian cancer. Taken together, these findings suggest a role of *RASAL2* as an oncogene in TNBC and ER-negative breast tumors as well as in aggressive ovarian tumors.

RASAL2 promotes TNBC tumorigenesis independently of its GAP activity. We next sought to test our hypothesis by experimentally determining the functional role of *RASAL2* in TNBC tumorigenesis. MDA-MB231-LN is a metastasis subline of MDA-MB-231 that is more invasive and shows a more protrusive morphology in the 3D Matrigel as compared with the parental MDA-MB-231 cells (Supplemental Figure 5, A and B). Consistent with the clinical samples, MDA-MB-231-LN cells were found to express more abundant *RASAL2* compared with the parental cells (Supplemental Figure 5C) and thus were chosen for the subsequent functional studies (hereafter referred to as MB231-LN). In an in vitro Matrigel invasion assay, *RASAL2* knockdown by 2 independent siRNAs markedly reduced the invasiveness of MB231-LN and BT-549 cells (Figure 3A) as well as SUM159PT and HS578T cells (Supplemental Figure 5D) but not the cell proliferation in monolayer culture (Figure 3A). The specificity of *RASAL2* knockdown on cell invasion was further confirmed by a rescue experiment using ectopic expression of *RASAL2* and a third siRNA targeting the 3′ UTR of *RASAL2* (Fig-

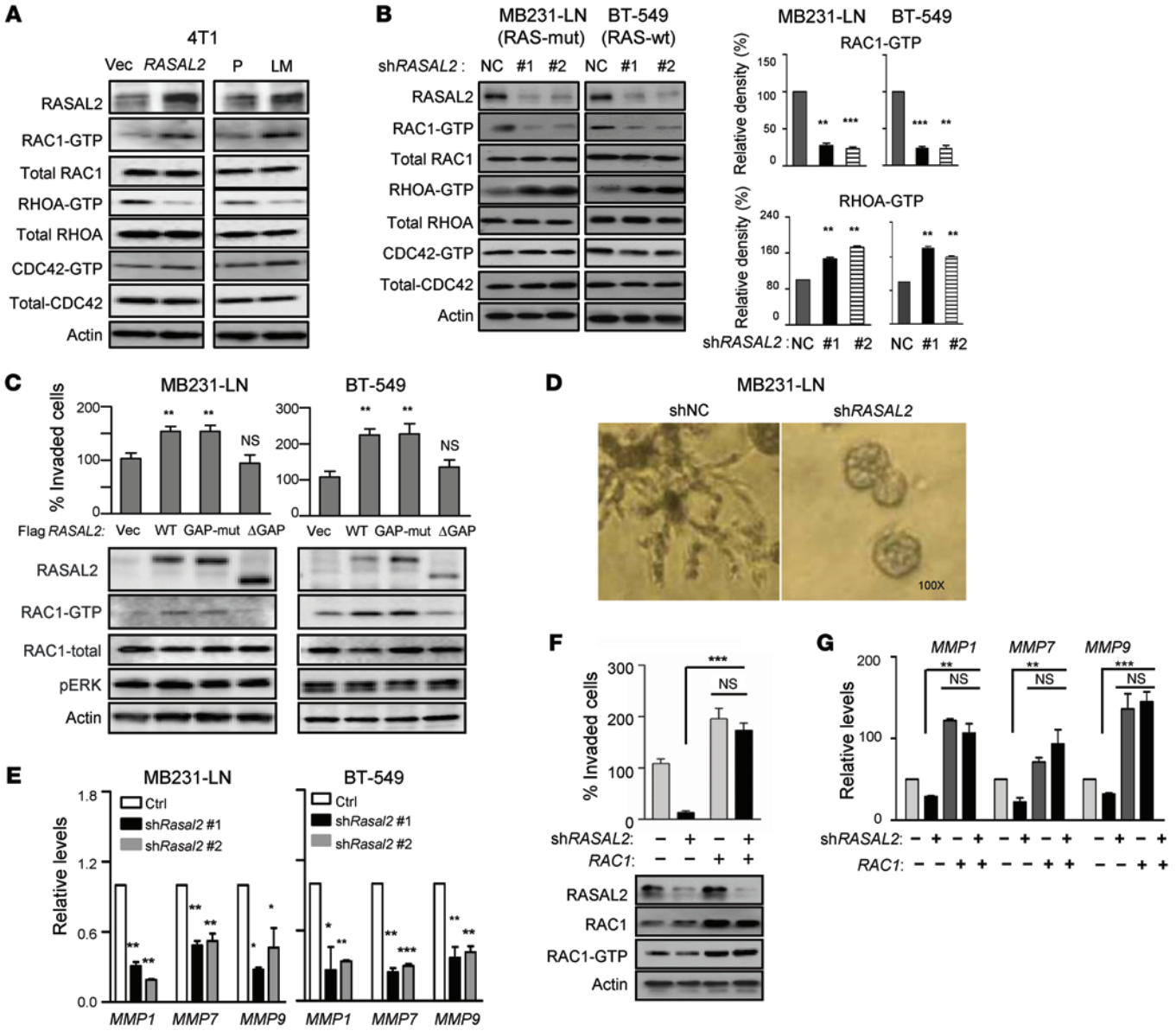

Figure 5. RASAL2 regulates TNBC cell invasion through modulating the activity of small GTPase RAC1. (**A**) Western blot showing levels of the active form of indicated small GTPases (GTP-bound RAC1, RHOA, and CDC42) and the total level of controls upon overexpression of ectopic *RASAL2* or endogenous *RASAL2* (LM) in 4T1 cells. P, parental 4T1 cells. (**B**) Western blots as in **A** of MB231-LN and BT-549 cells upon *RASAL2* depletion by shRNAs as indicated and quantification of the active RAC1 (RAC1-GTP) and active RHOA (RHOA-GTP) levels normalized to total RAC1 or RHOA levels by densitometry analysis. (**C**) Invasion assay and Western blot showing the levels of the active form of RAC1 and the total level of controls in cells expressing wild-type, GAP activity–deficient mutant, or GAP domain deletion mutant RASAL2. (**D**) Representative images of indicated MB231-LN cells cultured in 3D Matrigel. Original magnification, ×100. (**E**) qPCR analyses of *MMP1*, *MMP7*, and *MMP9* in indicated cell lines. (**F**) Invasion assay and Western blot showing the levels of the active form of RAC1 and the total level of controls in MB231-LN cells with indicated treatment. (**G**) qPCR analysis of *MMP1*, *MMP7*, and *MMP9* in MB231-LN cells with indicated treatment. The data shown represent mean ± SEM of 3 independent or replicate experiments. $^*P < 0.05$, $^{**}P < 0.01$, $^{***}P < 0.001$.

ure 3B). *RASAL2* knockdown also markedly reduced the migration of MB231-LN cells, as measured by a wound healing assay (Figure 3C) and 3D Matrigel growth (Figure 3D). In addition, *RASAL2* knockdown also reduced the cell properties associated with breast cancer cell stemness, including mammosphere-forming ability in a serum-free suspension cell culture (Figure 3E) and the $CD44^{hi}$ $CD24^{lo}$ cell population (Figure 3F). Together, these results indicate that RASAL2 is required to support the aggressive growth of TNBC cells, including invasion, migration, and self-renewal, though it was not necessarily required for the cell proliferation.

In luminal tumors, RASAL2 has been shown to act as a tumor-suppressive RAS-GAP protein, and its downregulation leads to the activation of RAS/MAPK signaling (28). Given the observed pro-oncogenic role of RASAL2 in TNBC and that depletion of *RASAL2* was able to inhibit the invasion capacity in both RAS wild-type (BT-549) and RAS mutant (MDA-MB-231) TNBC cells, we hypothesized that RASAL2 oncogenic activity in TNBC is independent of RAS-GAP activity. It has been shown that mutations of K417 and K567 in the GAP catalytic domain lead to the loss of catalytic activity of RASAL2 toward RAS/ERK signaling (28). To

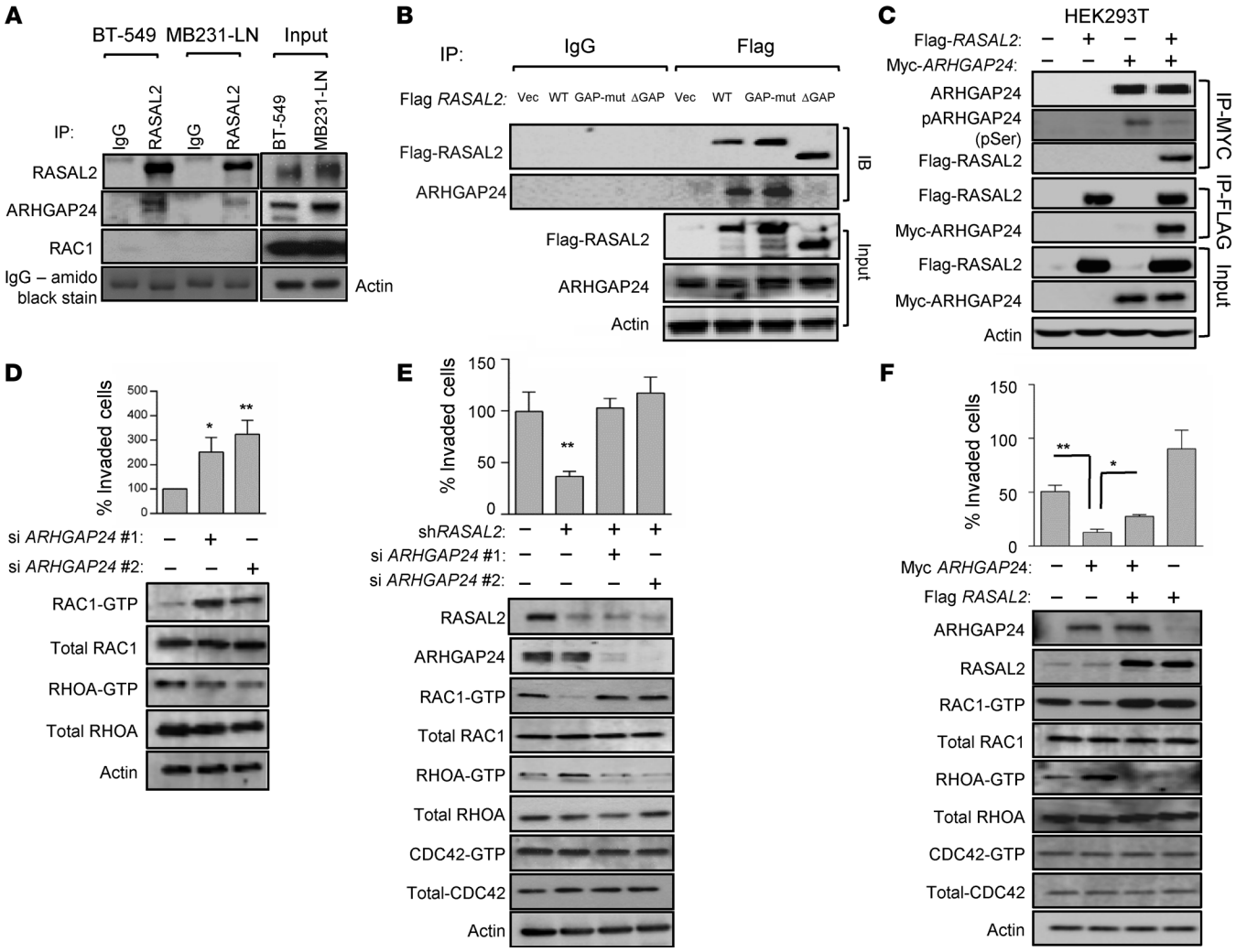

Figure 6. RASAL2 activates RAC1 through direct binding to and inhibiting of the RAC GAP protein, ARHGAP24. (**A**) Coimmunoprecipitation assays were performed with MB231-LN and BT-549 cells showing the endogenous *RASAL2* association with ARHGAP24 but not RAC1. (**B**) Coimmunoprecipitation assays were performed with BT-549 cells showing the ectopic wild-type and GAP activity–deficient mutant *RASAL2* association with ARHGAP24 but not the GAP domain deletion mutant. (**C**) Coimmunoprecipitation assays were performed with 293T cells expressing Myc-tagged *ARHGAP24*, Flag-tagged *RASAL2*, or both, and cells were probed with indicated antibodies. (**D**) Invasion assay of BT-549 cells treated with 2 independent *ARHGAP24* siRNAs and Western blot analysis of active and total levels of RAC1 and RHOA. (**E**) Invasion assay of BT-549 cells treated with *RASAL2* siRNA, *ARHGAP24* siRNAs, or both and Western blot analysis of active and total levels of RAC1 and RHOA in the same cells as above. (**F**) Invasion assay of BT-549 cells with single or double *RASAL2* and *ARHGAP24* ectopic expression, respectively, and Western blot analysis of the indicated proteins. The data shown represent mean ± SEM of 3 independent or replicate experiments. $^*P < 0.05$, $^{**}P < 0.01$.

test whether RAS-GAP activity is required for RASAL2 function in TNBC, we made a GAP activity–deficient mutant of RASAL2, together with a GAP domain deletion mutant, and performed the rescue experiment in RASAL2 knockdown cells. The results showed that the GAP activity–deficient mutant retained its activity to restore invasion upon RASAL2 knockdown in TNBC cells, indicating that GAP catalytic activity is dispensable for oncogenic RASAL2 function. In contrast, the GAP deletion mutant failed to do so, indicating that RASAL2 still required the presence of the GAP domain to exert its oncogenic function (Figure 3G).

To study RASAL2 function in vivo, we first made use of the basal-like 4T1 mouse mammary tumor cells and compared the expression levels of *RASAL2* and miR-203 in parental 4T1 cells and a metastatic subline derived from the lung metastasis (referred to as 4T1-LM) following mammary gland fat pad injection (Figure 4A). We found that while the expression of the mouse miR-203, which bears a sequence that is 100% identical to that of human miR-203, was decreased in 4T1-LM cells compared with the parental 4T1 cells, the expression of *RASAL2* was increased (Figure 4B), accompanied by an increased invasiveness of 4T1-LM cells (Supplemental Figure 6A). Since the mouse and the human RASAL2 protein sequences are over 96% identical, we next ectopically overexpressed human *RASAL2* in parental 4T1 cells and asked whether the ectopic RASAL2 is sufficient to increase invasion in vitro and metastasis in vivo. Indeed, ectopic overexpression of RASAL2 in 4T1 cells increased the invasiveness (Supplemental Figure 6B). Measurement of spontaneous lung metastasis through orthotopic transplant of 4T1 and 4T1 *RASAL2* cells into mammary gland fat pads of

NOD/SCID mice by bioluminescence imaging as well as lung tissue staining revealed that although the RASAL2 overexpression had little effect on the primary tumor growth (Figure 4C), it significantly increased the burden of lung metastasis (Figure 4D).

We further used MB231-LN cells that express a luciferase reporter to investigate the role of RASAL2 in TNBC metastasis. *RASAL2* knockdown in MB231-LN cells expressing a short hairpin RNA targeting *RASAL2* or the nontargeting control cells implanted in mouse mammary gland fat again produced no appreciable effect on primary tumor growth (Figure 4E) but significantly decreased the burden of lung metastasis (Figure 4F), which consequently resulted in prolonged survival of the tumor-bearing mice ($P = 0.008$) (Figure 4G).

Next, we evaluated the development of lung metastasis following the injection of MB231-LN cells via the mouse tail vein. In this model, *RASAL2* knockdown also significantly inhibited lung metastasis (Figure 4H) and prolonged the survival of tumor-bearing mice (Figure 4I). Although the effect was not as marked as that seen in orthotopic models, this showed that RASAL2 is also important in allowing circulating tumor cells to establish metastatic colonies, a later step of metastasis. Taken together, both of gain-of-function and lost-of-function in vivo studies demonstrate a crucial role for RASAL2 in driving TNBC metastasis.

RASAL2 acts to activate the small GTPase RAC1 for mesenchymal cell invasion. Previous studies have shown that some GAPs for one family of small GTPases can act to promote the activity of other families of small GTPases. For example, the RAS-GAP protein p120 RAS-GAP, also called RASA1, can activate the RHOA GTPase through interaction with and inhibition of the RHO-GAP protein DLC1 tumor suppressor (32). To determine whether this was the case with RASAL2, we examined whether RASAL2 was able to regulate the activities of the other small GTPases family members, including RAC1, RHOA, and CDC42, all known to promote cancer invasion and metastasis (33–36). Here, we found that, by affinity pull-down analysis of respective GTP-bound GTPases, *RASAL2* overexpression in 4T1 cells resulted in increased RAC1 activity (GTP-bound RAC1), decreased RHOA activity, and no change in CDC42 activity (Figure 5A). Conversely, *RASAL2* knockdown in MB231-LN and BT-549 cells led to reduction of RAC1 activity and increased RHOA activity (Figure 5B). In both above experiments, RASAL2 manipulations did not change RAS-GTP levels or downstream ERK phosphorylation (Supplemental Figure 6, C and D). In contrast, ectopic expression of RASAL2 in 2 luminal B breast cancer cell lines, BT474 and MB361, resulted in downregulation of RAS-GTP and ERK phosphorylation as well as decreased cell invasion and soft agar growth (Supplemental Figure 7, A–C). Moreover, both wild-type RASAL2 and GAP activity–deficient mutant RASAL2, but not GAP domain deletion mutant RASAL2, activated the RAC1 activity in TNBC (Figure 5C). By contrast, the tumor suppressor activity of RASAL2 in luminal BT474 and MB361 cells indeed requires RASAL2's GAP activity (Supplemental Figure 7D). These findings demonstrate a context-dependent role of RASAL2 in breast cancer.

RAC1 and RHOA are known to be mutually antagonistic, though both can promote cell invasion and motility through different mechanisms (37–39). While RAC1 drives mesenchymal motility, in which the cells are elongated, RHOA drives amoeboid motility, in which the cells are round (40–43). Consistent with this notion, we observed that, when *RASAL2* was knocked down and cultured in 3D Matrigel, MB231-LN cells underwent a change from an elongated morphology to a rounded form (Figure 5D). In addition, expression levels of several MMP family members, which are hallmark indicators of RAC1-driven mesenchymal motility (38, 44, 45), were markedly decreased upon *RASAL2* knockdown in TNBC cells (Figure 5E).

Critically, like RASAL2, ectopic RAC1 increased invasion and MMP expression and robustly rescued the RASAL2 knockdown effects (Figure 5, F and G), confirming a functional link between RASAL2 and RAC1. Collectively, these results provide evidence that RASAL2 promotes mesenchymal cell invasion in TNBC through activating RAC1 activity at large.

RASAL2 regulates RAC1 activity through binding to and antagonizing RAC1 GAP protein, ARHGAP24. Next, we investigated the molecular mechanism by which RASAL2 regulates RAC1 activity. RASAL2 did not coimmunoprecipitate with RAC1 (Figure 6A and data not shown), suggesting that RASAL2 may regulate RAC1 activity indirectly. As activity of small GTPases is often negatively regulated by its GAP proteins, we explored the possibility that RASAL2 may promote RAC1 activity by antagonizing a RAC1 GAP protein. Two RAC1 GAPs, ARHGAP24 (also known as FilGAP) and ARHGAP22, have been previously shown to be involved in breast cancer cell invasion and motility (46–48) and thus were investigated for their potential roles in mediating RASAL2 activity toward RAC1. To do this, we first determined whether RASAL2 can be found in the same protein complex with ARHGAP24 or ARHGAP22. In both MB231-LN and BT-549 cells, we found that the endogenous RASAL2 coimmunoprecipitated with endogenous ARHGAP24 but not ARHGAP22 in TNBC cells (Figure 6A and data not shown), and this interaction was not detected in luminal cells (Supplemental Figure 7E). Furthermore, both wild-type RASAL2 and GAP activity–deficient mutant RASAL2 interacted with ARHGAP24, while GAP deletion mutant RASAL2 did not (Figure 6B). This result shows that RASAL2 requires the GAP domain but not the GAP activity to interact with ARHGAP24.

We next investigated whether RASAL2 interaction with ARHGAP24 affects its activity. It has been shown that serine phosphorylation of ARHGAP24 promotes its activity to regulate RAC1 (47). We found that, in cells transfected with ARHGAP24, RASAL2, or both, immunoprecipitated ARHGAP24 showed reduced serine phosphorylation in RASAL2 and ARHGAP24 cotransfected cells compared with cells transfected with ARHGAP24 alone (Figure 6C). This finding supports that RASAL2 interaction with ARHGAP24 negatively regulates ARHGAP24 activity.

Finally, we investigated the functional interplay between RASAL2 and ARHGAP24 in regulating RAC1 activity and cell invasiveness. Consistent with RAC1 GAP proteins, ARHGAP24 knockdown in TNBC cells resulted in enhanced activity of RAC1 and invasion capacity (Figure 6D) and thus restored the RAC1 activity and cell invasion suppressed upon RASAL2 knockdown (Figure 6E). Conversely, ectopic overexpression of ARHGAP24 in TNBC cells resulted in suppression of cell invasion and RAC1 activity, which were rescued at least partially by coexpression of RASAL2 (Figure 6F). Collectively, these results support that RASAL2 enhances RAC1 activity toward TNBC cell invasion, at least in part, through binding to and antagonizing the RAC1 GAP protein ARHGAP24.

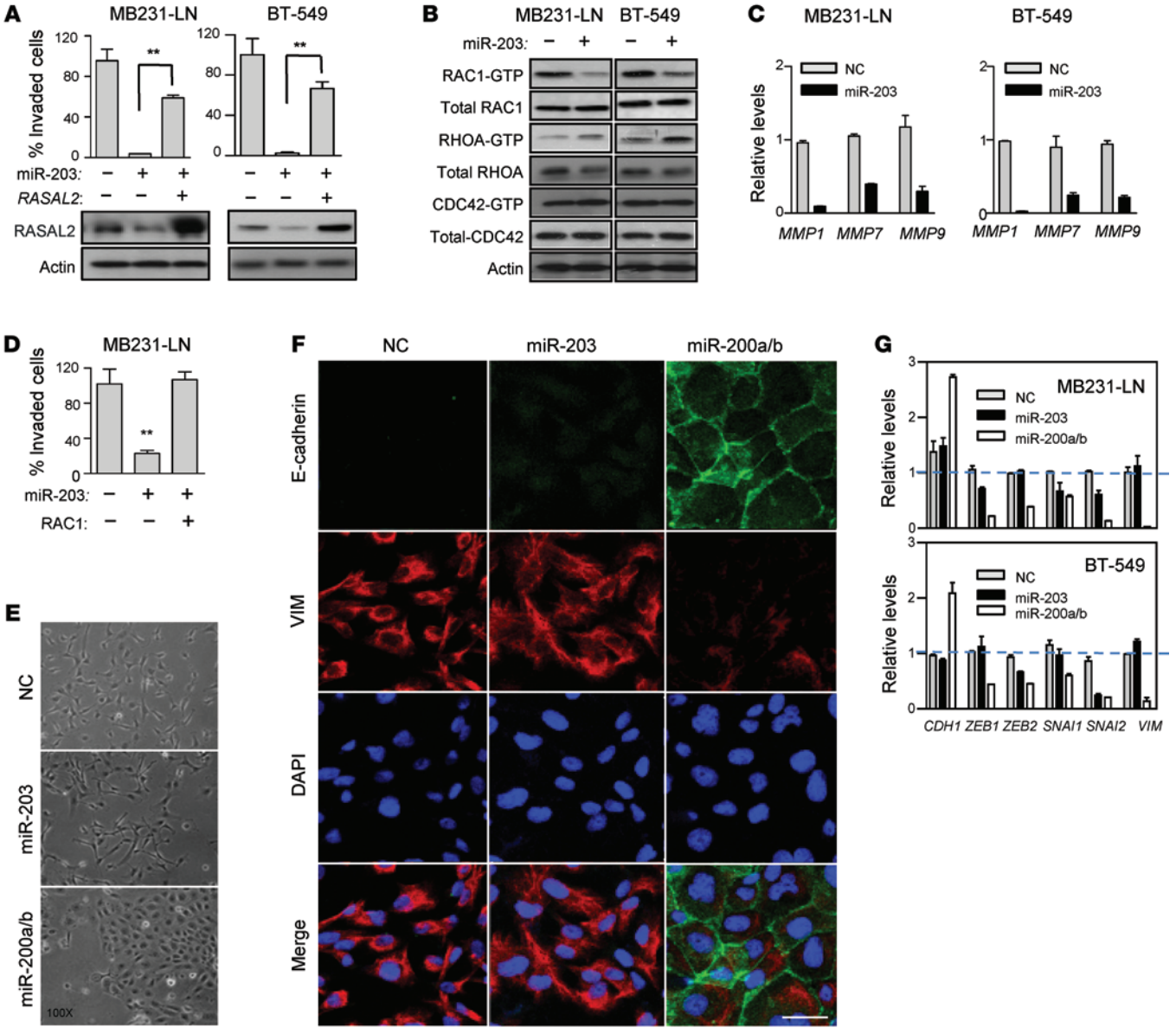

Figure 7. miR-203–targeted RASAL2/RAC1 regulates mesenchymal invasion, without affecting EMT. (**A**) Invasion assay and Western blot analysis in MB231-LN and BT-549 cells treated with miR-203 in the presence or absence of ectopic *RASAL2*. (**B**) Western blot analysis of indicated proteins in cells treated with miR-203. (**C**) qPCR analysis of *MMP1*, *MMP7*, and *MMP9* in cells treated with miR-203. (**D**) Invasion assay in MB231-LN cells ectopically expressing RAC1 and miR-203. (**E**) Cell morphology changes of MB231-LN cells treated with miR-203 or miR-200a/b. Original magnification, ×100. (**F**) Confocal immunofluorescence staining of E-cadherin and vimentin in MB231-LN cells treated with miR-203 and miR-200a/b. Scale bar: 20 μm. (**G**) qPCR analysis of EMT-related genes. The data shown represent mean ± SEM of 3 independent or replicate experiments. $^{**}P < 0.01$.

miR-203–targeted RASAL2/RAC1 regulates mesenchymal invasion, without affecting EMT. miRNAs act pleiotropically by targeting multiple gene targets. In particular, miR-203 has been previously shown to inhibit tumor cell invasion and suppress EMT in lung and prostate cancer cells by targeting *ZEB2* and *SNA12* (22, 49). Thus, this raised a question of whether miR-203 inhibits TNBC cell invasion via targeting RASAL2/ARHGAP23/RAC1 and/or alternatively via targeting EMT. To address this, rescue experiments using ectopic RASAL2/RAC1 in miR-203–treated cells were performed. In both MB231-LN and BT-549 cells, ectopic RASAL2 expression was able to rescue the anti-invasive effect of miR-203 (Figure 7A). Consistent with it being an upstream inhibitor of RASAL2, miR-203 treatment in TNBC cells also resulted in suppression of RAC1-GTP (Figure 7B) as well as MMPs (Figure 7C). Similarly, like RASAL2, ectopic RAC1 was also able to rescue the anti-invasive effect of miR-203 (Figure 7D). These findings confirmed a role of RASAL2/RAC1 as a functional target of miR-203 in TNBC cell invasion.

We next assessed whether miR-203 is able to affect the EMT of TNBC cells. To this end, we first examined the morphological changes of MB231-LN cells upon miR-203 treatment. For comparison, miR-200a/b, known to inhibit EMT in TNBC cells (16, 17), was used as a control. The results showed that miR-200a/b, but not miR-203, was able to induce an apparent epithelial mor-

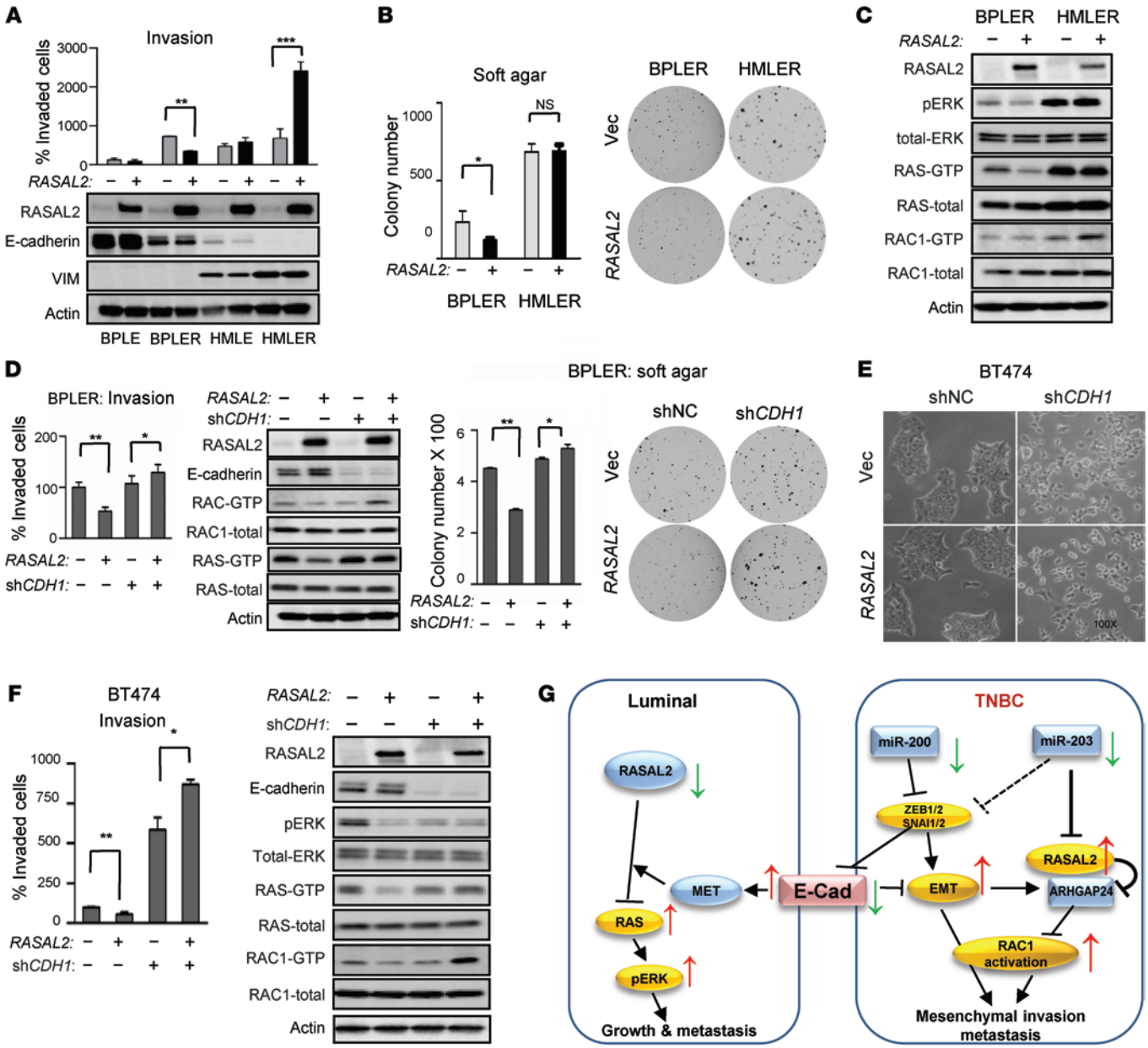

Figure 8. The context-dependent role of RASAL2 in breast cancer is dependent on EMT status. (**A**) Invasion assay in BPLE, BPLER, HMLE, and HMLER cells with stable ectopic *RASAL2* expression and Western blot analysis of protein levels. (**B**) Soft agar growth of indicated cell lines. (**C**) Western blot showing the levels of the active form of indicated small GTPases (GTP-bound RAC1 and RAS) and the total levels of controls upon ectopic *RASAL2* expression in BPLER and HMLER cells. (**D**) Invasion assay and Western blot showing the levels of the active form of RAC1 and the total levels of controls in BPLER cells expressing ectopic *RASAL2* with or without *CDH1* knockdown and soft agar assay of the same cell lines. (**E**) BT474 cell morphology change upon *CDH1* knockdown. Original magnification, ×100. (**F**) Invasion assay and Western blot showing indicated proteins in BT474 cells expressing ectopic *RASAL2* with or without *CDH1* knockdown. (**G**) A schematic model showing context-dependent roles of RASAL2 in breast cancer. The data shown represent mean ± SEM of 3 independent or replicate experiments. $^{*}P < 0.05$, $^{**}P < 0.01$, $^{***}P < 0.001$.

phology suggestive of EMT reversal (Figure 7E), which was further confirmed by confocal imaging analysis of the epithelial marker E-cadherin (*CDH1*) and the mesenchymal marker vimentin (*VIM*) (Figure 7F). Further assessment of a panel of EMT-related genes by qPCR showed that, in both MB231-LN and BT-549 cells, miR-200a/b treatment induced the expression of *CDH1* and decreased the expression of *VIM*, *ZEB1/2*, and *SNAI1/2*, while miR-203 treatment did not induce such molecular changes, though it modestly decreased *SNAI2* (also known as *SLUG*) expression (Figure 7G). Thus, compared with miR-200a/b, miR-203 does not seem to be a strong EMT regulator in TNBC. Taken together, these results support the conclusion that the anti-invasive effect of miR-203 in TNBC was mediated through targeting RASAL2/RAC1 activity, rather than targeting EMT.

Context-dependent roles of RASAL2 in breast cancer are dependent on EMT status. Because RASAL2 is tumor suppressive in luminal breast cancer but oncogenic in TNBC, we next sought to determine whether EMT status plays a role in this context-dependent

functional switch. This hypothesis first arose from our observation that, in nonmesenchymal (epithelial) TNBC cell lines, such as HCC1806 and HCC1937, in which RASAL2 was equally expressed at levels as high as those in mesenchymal TNBC cells, RASAL2 knockdown failed to inhibit the cell invasion (Supplemental Figure 8A). As previously reported and also shown here, miR-200a/b was expressed abundantly in luminal or nonmesenchymal TNBC cells but not in mesenchymal TNBC cells (Supplemental Figure 8B) (24). We asked whether miR-200a/b inhibition in the nonmesenchymal TNBC cells would facilitate EMT induction and thus stimulate RASAL2 activity in these cells. Indeed, antagomir inhibition of miR-200a/b markedly induced mesenchymal markers in HCC1806 and HCC1937 cells (Supplemental Figure 8C) and increased cell invasion, which was then abolished by *RASAL2* knockdown (Supplemental Figure 8D). This initial finding raised the possibility that an EMT status is probably a prerequisite for RASAL2 to function as an oncogene.

To directly address this issue, we took the advantage of a series of immortalized (BPLE and HMLE) and respectively transformed (BPLER and HMLER) human mammalian cell lines that express differential luminal or basal markers. BPLE and BPLER cells expressed more luminal epithelial gene markers and expressed high levels of E-cadherin but low levels of vimentin, while HMLE and HMLER cells expressed more basal epithelial gene markers and showed expression levels opposite of those of BPLE and BPLER cells for E-cadherin and vimentin (refs. 50, 51, and Figure 8A). Consistent with the context-dependent role of RASAL2, as we predicted, ectopic expression of RASAL2 in more luminal-like BPLE and BPLER cells reduced cell invasion (Figure 8A) and soft agar growth (Figure 8B), while it enhanced cell invasion of HMLER cells, though it did not change much of its soft agar growth (Figure 8, A and B). Consistently, we saw reduced RAS-GTP and ERK phosphorylation upon ectopic RASAL2 expression in BPLER cells but increased RAC1-GTP in HMLER cells (Figure 8C). Intriguingly, E-cadherin knockdown in BPLER cells abolished the inhibitory effects of ectopic RASAL2 on invasion, growth, RAS-GTP, and ERK phosphorylation and stimulated ectopic RASAL2 to activate RAC-GTP (Figure 8D). Moreover, in luminal B breast cancer BT474 cells, E-cadherin knockdown induced an EMT morphology (Figure 8E), and again, under this condition, ectopic RASAL2 lost its ability to suppress RAS activity and cell invasion in BT474 cells; rather, it increased the cell invasion and RAC1 activity (Figure 8F). Collectively, these findings demonstrate that induction of mesenchymal status is inhibitory for the tumor-suppressive RAS-GAP activity but required for the oncogenic activity of RASAL2 to promote RAC1 activity and invasion capacity. These findings have thus provided a mechanistic insight into the context-dependent role of RASAL2 in breast cancer, as shown in a proposed model (Figure 8G).

Discussion

Dissecting the molecular pathways that drive breast cancer invasion and metastasis remains crucial to understanding the disease progression and development of therapeutic strategies. Here, we provide evidence for an anti-invasive miR-203–targeted RASAL2/RAC1 pathway in TNBC invasion and metastasis. In contrast to a previously described role as a tumor suppressor in luminal breast tumors via targeting RAS activity (28), *RASAL2* is overexpressed in TNBC, in which it predicts poor disease outcomes and directs mesenchymal invasion and metastasis through promoting small GTPase RAC1 activity. Our study demonstrates the context dependency of *RASAL2* in breast cancer and provides mechanistic insights into the oncogenic activity of *RASAL2* in TNBC.

Our findings in TNBC appear to be in contrast with that of a previous finding in luminal B breast cancer, in which *RASAL2* was found to act as a RAS-GAP tumor suppressor whose downregulation due to promoter hypermethylation resulted in inactivation of RAS signaling and increased growth and metastasis (28). As opposed to the downregulation of *RASAL2* in the luminal B subtype, we found that *RASAL2* was overexpressed in 30% to 40% of TNBC and ER-negative tumors, and this downregulation could be due to a loss of miR-203 expression, as we identified here, and could also be in part due to possible gene amplification, as revealed by TCGA genomic analysis. In a meta-analysis of breast cancer, including multiple cohorts, we found that *RASAL2* expression was positively associated with poorer disease outcomes in TNBC and ER-negative tumors but had an opposite trend in luminal tumors. In addition, higher *RASAL2* expression was found to be associated with increased incidence of metastasis and recurrence in TNBC or ER-negative tumors, further supporting its role in disease progression and possibly also chemoresistance. Importantly, *RASAL2* upregulation and gene copy number gain were also found in high-grade serous ovarian cancer, which has been recently found to share a similar molecular portrait to TNBC through large-scale genomic analyses (30), and were also associated with metastatic progression and poor outcomes in multiple ovarian cancer cohorts. This suggests that the oncogenic role of *RASAL2* is not limited to TNBC. The contradictory roles of *RASAL2* in TNBC and luminal cancers underscore an important context dependency of *RASAL2* function in human cancers.

Experimentally, both gain-of-function and loss-of-function analyses in vitro and in vivo have demonstrated the oncogenic role of *RASAL2* in TNBC invasion and metastasis. Mechanistically, we show that the oncogenic function of *RASAL2* in TNBC is irrelevant to RAS status, as RASAL2 depletion attenuates the invasive phenotype in both RAS wild-type and mutated TNBC cells and does not affect RAS activity or the downstream MAPK signaling in TNBC. Rather, RASAL2 deletion effectively abolished the activity of RAC1, which is known to be involved in mesenchymal cell invasion (38, 44, 52, 53). We further demonstrate that the ability of *RASAL2* to regulate RAC1 is through binding to and antagonizing RAC1 GTPase-activating protein ARHGAP24, which, in the absence of RASAL2, functions to inhibit RAC1 activity.

We show that the context dependency of RASAL2 in breast cancer depends on the EMT status. This is demonstrated by using well-defined human mammalian epithelial cell line models that express different mesenchymal and epithelial markers. RASAL2 acts as an oncogene to promote invasion and RAC1 activity in basal HMLER cells with reduced E-cadherin but functions as a tumor suppressor to reduce growth and RAS activity in more luminal BPLER cells that express abundant E-cadherin. E-cadherin knockdown in BPLER cells abolished the tumor suppressor activity of RASAL2 and stimulated it to induce RAC1 activity. The same was also seen in luminal breast cancer cell line BT474, in which inducing EMT by E-cadherin knockdown inactivates the RASAL2

tumor suppressor activity. Thus, the molecular traits of EMT, such as E-cadherin, seem to be crucial for RASAL2 to be oncogenic but inhibitory for its tumor suppressor activity. Given the functional complexity and heterogeneity of molecular cancer pathways, it perhaps not so surprising that such paradoxes are often found in human cancers. This phenomenon seems to resemble TGF-β signaling, which acts as an oncogene in basal breast tumors, in which it promotes EMT and metastasis, and acts as a tumor suppressor in luminal tumors, in which it is downregulated (54, 55).

Although miR-203 has been previously shown to inhibit EMT by targeting *ZEB2* in lung and prostate cancers, miR-203 does not appear to directly regulate EMT in TNBC because, unlike miR-200, miR-203 did not reverse EMT-associated morphological and molecular changes in TNBC cells. Thus, miR-203 acts to repress TNBC invasion independently of EMT modulation, as seen in other cancers. Although loss of miR-203 does not seem to induce the EMT process itself, it potentiates mesenchymal invasion in TNBC cells through modulating RASAL2/RAC1 activity. This is consistent with the previous finding that RAC1 activation mediates motility of cancer cells undergoing EMT (56). Thus, we propose a model in which the combined loss of miR-200s and miR-203 in TNBC work collaboratively to facilitate invasion and metastasis in TNBC.

Although EMT appears to be rare within primary TNBC tumors, it is highly enriched (up to 100%) in circulating breast tumor cells of patients with TNBC (57). Given the strong association of circulating tumor cells with breast cancer metastatic progression (57), the discovery of miR-203–targeted RASAL2/RAC1 as a crucial regulator of mesenchymal invasion provides a rational for therapeutic targeting of *RASAL2* for TNBC metastasis. This can be developed potentially into a highly needed therapeutic target in TNBC, for which poor clinical outcome is compounded by the absence of any targeted therapeutics. Further studies to evaluate the potential of *RASAL2* as both a predictive and prognostic marker in TNBC will provide more accurate stratification and also a means of reducing disease recurrence in the 30% to 40% of patients with TNBC who develop early relapse despite chemotherapy.

Methods

Please refer to the Supplemental Methods section for more detailed information.

Cell lines and reagents. The breast cancer cell lines used in this study were purchased from ATCC. BPLE and BPLER cells were gifts from Robert Weinberg (Whitehead Institute for Biomedical Research, Cambridge, Massachusetts, USA) and were maintained in WIT-T Culture Medium (Stemgent). MB231-LN (MDA-MB-231-Luc-D3H2LN) cells were purchased from Perkin Elmer. Constructs of ectopic RASAL2 expression, siRNAs, and shRNAs for *RASAL2* knockdown can be found in the Supplemental Methods. For primers and siRNA sequences, see Supplemental Table 2.

miRNA profiling and quantitative RT-PCR validation. Total RNAs were isolated and purified with the Qiagen miRNeasy Mini Kit (catalog no. 217004). The miRNA expression array hybridization was performed using Agilent Human miRNA Microarray Kit V3 (Agilent, catalog no. G4470C), and data analysis was performed as previously described (24). Detailed information and additional assays for validation of RT-PCR transcription can be found in Supplemental Methods.

IHC. Breast cancer TMA slides (BR1505 and BRM961) were purchased from USA Biomax. RASAL2 expression was probed with RASAL2 antibody (Novus Biologicals, catalog no. NBP1-82579). Additional details of IHC are provided in the Supplemental Methods.

Statistics. All in vitro experiments were repeated at least 3 times, unless stated otherwise, and data are reported as mean ± SEM. To normalize the expression of each patient cohort, expression values were normalized by calculating the z-score for each independent data set. The differences were assessed using 2-tailed Student's *t* test or 1-way ANOVA for multiple group comparisons using GraphPad Prism 6 software. Animal study survival curves were plotted using Kaplan-Meier analysis, and the statistical parameters were calculated by log-rank (Mantel-Cox) test using Graphpad Prism. In all statistical tests, $P \leq 0.05$ was considered significant unless stated otherwise.

Study approval. Human tissue samples were provided by John Wayne Cancer Institute and Tan Tock Seng Hospital, and studies with these samples were approved by institutional review boards of each institution, respectively. Informed written consent was obtained from each individual who agreed to provide tissue for research purposes. All animal studies were conducted in compliance with animal protocols approved by the A*STAR-Biopolis Institutional Animal Care and Use Committee of Singapore.

Accession Number. Original microarray data were deposited in the NCBI's Gene Expression Omnibus (GEO accession no. GSE62022).

Acknowledgments

We thank the histopathology department of the Institute of Molecular and Cell Biology, A*STAR, for their service in IHC staining and analysis. We thank Mei Yee Aau for microarray hybridization and Chew Hooi Wong for assistance with tumorsphere assay. We thank Robert Weinberg's lab (Whitehead Institute for Biomedical Research, Cambridge, Massachusetts, USA) for providing BPLE/BPLER and HMLE/HMLER cell lines and Wai Leong Tam for technical guidance. This work was supported by A*STAR of Singapore, The National Healthcare Group clinician-scientist career scheme (CSCS/12004 to E.Y. Tan), the Margie and Robert E. Petersen Foundation, the ABC Foundation, and the Leslie and Susan Gonda (Goldschmied) Foundation (to D.S.B. Hoon, D.M. Marzese, and J. Wang).

Address correspondence to: Qiang Yu, Cancer Therapeutics and Stratified Oncology, Genome Institute of Singapore, 60 Biopolis Street, 02-01, Singapore 138672. Phone: 65.6478.8127; E-mail: yuq@gis.a-star.edu.sg.

1. Carey L, Winer E, Viale G, Cameron D, Gianni L. Triple-negative breast cancer: disease entity or title of convenience? *Nat Rev Clin Oncol*. 2010;7(12):683–692.
2. Foulkes WD, Smith IE, Reis-Filho JS. Triple-negative breast cancer. *N Engl J Med*. 2010;363(20):1938–1948.
3. Berrada N, Delaloge S, Andre F. Treatment of triple-negative metastatic breast cancer: toward individualized targeted treatments or chemosensitization? *Ann Oncol*. 2010;21(suppl 7):vii30–vii35.
4. Gupta GP, Massague J. Cancer metastasis: building a framework. *Cell*. 2006;127(4):679–695.
5. Joyce JA, Pollard JW. Microenvironmental regulation of metastasis. *Nat Rev Cancer*. 2009;9(4):239–252.
6. Pencheva N, Tavazoie SF. Control of metastatic progression by microRNA regulatory networks.

Nat Cell Biol. 2013;15(6):546–554.
7. Nicoloso MS, Spizzo R, Shimizu M, Rossi S, Calin GA. MicroRNAs — the micro steering wheel of tumour metastases. *Nat Rev Cancer*. 2009;9(4):293–302.
8. Valastyan S, et al. A pleiotropically acting microRNA, miR-31, inhibits breast cancer metastasis. *Cell*. 2009;137(6):1032–1046.
9. Yu F, et al. let-7 regulates self renewal and tumorigenicity of breast cancer cells. *Cell*. 2007;131(6):1109–1123.
10. Iorio MV, et al. MicroRNA gene expression deregulation in human breast cancer. *Cancer Res*. 2005;65(16):7065–7070.
11. Ma L, Teruya-Feldstein J, Weinberg RA. Tumour invasion and metastasis initiated by microRNA-10b in breast cancer. *Nature*. 2007;449(7163):682–688.
12. Tavazoie SF, et al. Endogenous human microRNAs that suppress breast cancer metastasis. *Nature*. 2008;451(7175):147–152.
13. Yang X, et al. miR-449a and miR-449b are direct transcriptional targets of E2F1 and negatively regulate pRb-E2F1 activity through a feedback loop by targeting CDK6 and CDC25A. *Genes Dev*. 2009;23(20):2388–2393.
14. Zhang Y, et al. miR-126 and miR-126* repress recruitment of mesenchymal stem cells and inflammatory monocytes to inhibit breast cancer metastasis. *Nat Cell Biol*. 2013;15(3):284–294.
15. Bracken CP, Gregory PA, Khew-Goodall Y, Goodall GJ. The role of microRNAs in metastasis and epithelial-mesenchymal transition. *Cell Mol Life Sci*. 2009;66(10):1682–1699.
16. Gregory PA, et al. The miR-200 family and miR-205 regulate epithelial to mesenchymal transition by targeting ZEB1 and SIP1. *Nat Cell Biol*. 2008;10(5):593–601.
17. Korpal M, Lee ES, Hu G, Kang Y. The miR-200 family inhibits epithelial-mesenchymal transition and cancer cell migration by direct targeting of E-cadherin transcriptional repressors ZEB1 and ZEB2. *J Biol Chem*. 2008;283(22):14910–14914.
18. Chaffer CL, Weinberg RA. A perspective on cancer cell metastasis. *Science*. 2011;331(6024):1559–1564.
19. Png KJ, Halberg N, Yoshida M, Tavazoie SF. A microRNA regulon that mediates endothelial recruitment and metastasis by cancer cells. *Nature*. 2012;481(7380):190–194.
20. Ryu S, et al. Suppression of miRNA-708 by polycomb group promotes metastases by calcium-induced cell migration. *Cancer Cell*. 2013;23(1):63–76.
21. Cao Q, et al. Coordinated regulation of polycomb group complexes through microRNAs in cancer. *Cancer Cell*. 2011;20(2):187–199.
22. Saini S, et al. Regulatory role of mir-203 in prostate cancer progression and metastasis. *Clin Cancer Res*. 2011;17(16):5287–5298.
23. Taube JH, et al. Epigenetic silencing of microRNA-203 is required for EMT and cancer stem cell properties. *Sci Rep*. 2013;3:2687.
24. Lee ST, et al. Protein tyrosine phosphatase UBASH3B is overexpressed in triple-negative breast cancer and promotes invasion and metastasis. *Proc Natl Acad Sci U S A*. 2013;110(27):11121–11126.
25. Ringner M, Fredlund E, Hakkinen J, Borg A, Staaf J. GOBO: gene expression-based outcome for breast cancer online. *PLoS One*. 2011;6(3):e17911.
26. Rhodes DR, et al. Oncomine 3.0: genes, pathways, and networks in a collection of 18,000 cancer gene expression profiles. *Neoplasia*. 2007;9(2):166–180.
27. Perou CM, et al. Molecular portraits of human breast tumours. *Nature*. 2000;406(6797):747–752.
28. McLaughlin SK, et al. The RasGAP gene, RASAL2, is a tumor and metastasis suppressor. *Cancer Cell*. 2013;24(3):365–378.
29. Esserman LJ, et al. Pathologic complete response predicts recurrence-free survival more effectively by cancer subset: results from the I-SPY 1 TRIAL — CALGB 150007/150012, ACRIN 6657. *J Clin Oncol*. 2012;30(26):3242–3249.
30. Cancer Genome Atlas Network. Comprehensive molecular portraits of human breast tumours. *Nature*. 2012;490(7418):61–70.
31. Meyniel JP, et al. A genomic and transcriptomic approach for a differential diagnosis between primary and secondary ovarian carcinomas in patients with a previous history of breast cancer. *BMC Cancer*. 2010;10:222.
32. Yang XY, Guan M, Vigil D, Der CJ, Lowy DR, Popescu NC. p120Ras-GAP binds the DLC1 Rho-GAP tumor suppressor protein and inhibits its RhoA GTPase and growth-suppressing activities. *Oncogene*. 2009;28(11):1401–1409.
33. Citterio C, et al. The rho exchange factors vav2 and vav3 control a lung metastasis-specific transcriptional program in breast cancer cells. *Sci Signal*. 2012;5(244):ra71.
34. Krauthammer M, et al. Exome sequencing identifies recurrent somatic RAC1 mutations in melanoma. *Nat Genet*. 2012;44(9):1006–1014.
35. Myant KB, et al. ROS production and NF-κB activation triggered by RAC1 facilitate WNT-driven intestinal stem cell proliferation and colorectal cancer initiation. *Cell Stem Cell*. 2013;12(6):761–773.
36. Sosa MS, et al. Identification of the Rac-GEF P-Rex1 as an essential mediator of ErbB signaling in breast cancer. *Mol Cell*. 2010;40(6):877–892.
37. Burridge K, Wennerberg K. Rho and Rac take center stage. *Cell*. 2004;116(2):167–179.
38. Parri M, Chiarugi P. Rac and Rho GTPases in cancer cell motility control. *Cell Commun Signal*. 2010;8:23.
39. Sahai E, Marshall CJ. RHO-GTPases and cancer. *Nat Rev Cancer*. 2002;2(2):133–142.
40. Kulkarni SV, Gish G, van der Geer P, Henkemeyer M, Pawson T. Role of p120 Ras-GAP in directed cell movement. *J Cell Biol*. 2000;149(2):457–470.
41. Mack NA, Whalley HJ, Castillo-Lluva S, Malliri A. The diverse roles of Rac signaling in tumorigenesis. *Cell Cycle*. 2011;10(10):1571–1581.
42. Pignatelli J, Tumbarello DA, Schmidt RP, Turner CE. Hic-5 promotes invadopodia formation and invasion during TGF-β-induced epithelial-mesenchymal transition. *J Cell Biol*. 2012;197(3):421–437.
43. Sanz-Moreno V, et al. Rac activation and inactivation control plasticity of tumor cell movement. *Cell*. 2008;135(3):510–523.
44. Kessenbrock K, Plaks V, Werb Z. Matrix metalloproteinases: regulators of the tumor microenvironment. *Cell*. 2010;141(1):52–67.
45. Overall CM, Kleifeld O. Tumour microenvironment — opinion: validating matrix metalloproteinases as drug targets and anti-targets for cancer therapy. *Nat Rev Cancer*. 2006;6(3):227–239.
46. Ehrlicher AJ, Nakamura F, Hartwig JH, Weitz DA, Stossel TP. Mechanical strain in actin networks regulates FilGAP and integrin binding to filamin A. *Nature*. 2011;478(7368):260–263.
47. Ohta Y, Hartwig JH, Stossel TP. FilGAP, a Rho- and ROCK-regulated GAP for Rac binds filamin A to control actin remodelling. *Nat Cell Biol*. 2006;8(8):803–814.
48. Saito K, Ozawa Y, Hibino K, Ohta Y. FilGAP, a Rho/Rho-associated protein kinase-regulated GTPase-activating protein for Rac, controls tumor cell migration. *Mol Biol Cell*. 2012;23(24):4739–4750.
49. Garofalo M, et al. EGFR and MET receptor tyrosine kinase-altered microRNA expression induces tumorigenesis and gefitinib resistance in lung cancers. *Nat Med*. 2012;18(1):74–82.
50. Visone R, et al. MicroRNAs (miR)-221 and miR-222, both overexpressed in human thyroid papillary carcinomas, regulate p27Kip1 protein levels and cell cycle. *Endocr Relat Cancer*. 2007;14(3):791–798.
51. Iorio MV, et al. MicroRNA signatures in human ovarian cancer. *Cancer Res*. 2007;67(18):8699–8707.
52. Spano D, Heck C, De Antonellis P, Christofori G, Zollo M. Molecular networks that regulate cancer metastasis. *Semin Cancer Biol*. 2012;22(3):234–249.
53. Symons M, Segall JE. Rac and Rho driving tumor invasion: who's at the wheel? *Genome Biol*. 2009;10(3):213.
54. Bloomston M, et al. MicroRNA expression patterns to differentiate pancreatic adenocarcinoma from normal pancreas and chronic pancreatitis. *JAMA*. 2007;297(17):1901–1908.
55. Visone R, et al. Specific microRNAs are downregulated in human thyroid anaplastic carcinomas. *Oncogene*. 2007;26(54):7590–7595.
56. Yang WH, et al. RAC1 activation mediates Twist1-induced cancer cell migration. *Nat Cell Biol*. 2012;14(4):366–374.
57. Yu M, et al. Circulating breast tumor cells exhibit dynamic changes in epithelial and mesenchymal composition. *Science*. 2013;339(6119):580–584.